European Radiology (2019) 29:2272–2282
https://doi.org/10.1007/s00330-018-5882-4

MAGNETIC RESONANCE

Prediction of sorafenib treatment–related gene expression for hepatocellular carcinoma: preoperative MRI and histopathological correlation

Zhi Dong[1] · Kun Huang[1,2] · Bing Liao[3] · Huasong Cai[1] · Yu Dong[3] · Mengqi Huang[1] · Xiaoqi Zhou[1] · Yingmei Jia[1] · Ling Xu[4] · Yanji Luo[1] · Zi-Ping Li[1] · Shi-Ting Feng[1]

Received: 11 September 2018 / Revised: 19 October 2018 / Accepted: 9 November 2018 / Published online: 13 December 2018

Abstract

Purpose To investigate the feasibility of prediction for targeted therapy-related gene expression in hepatocellular carcinoma (HCC) using preoperative gadoxetic acid-enhanced magnetic resonance imaging (MRI).

Materials and methods Ninety-one patients (81 men, mean age 53.9 ± 12 years) with solitary HCC who underwent preoperative enhanced MRI were retrospectively analyzed. Features including tumor size, signal homogeneity, tumor capsule, tumor margin, intratumoral vessels, peritumor enhancement, peritumor hypointensity, signal intensity ratio on DWI, T1 relaxation times, and the reduction rate between pre- and post-contrast enhancement images were assessed. The operation and histopathological evaluation were performed within 2 weeks after MRI examination (mean time 7 days). The expression levels of *BRAF, RAF1*, *VEGFR2*, and *VEGFR3* were evaluated. The associations between these imaging features and gene expression levels were investigated.

Results Tumor incomplete capsules or non-capsules ($p = 0.001$) and intratumoral vessels ($p = 0.002$) were significantly associated with *BRAF* expression, and tumor incomplete capsules or non-capsules ($p = 0.001$) and intratumoral vessels ($p = 0.013$) with *RAF1* expression. There was no significant association between the expression of *VEGFR2*, *VEGFR3*, and all examined MRI features. Multivariate logistic regression showed that incomplete tumor capsule ($p = 0.002$) and non-capsule ($p = 0.004$) were independent risk factors of HCC with high *BRAF* expression; incomplete tumor capsule ($p < 0.001$) and non-capsule ($p = 0.040$) were independent risk factors of HCC with high *RAF1* expression.

Conclusion The presence of incomplete capsule or intratumoral vessels and the absence of capsule are potential indicators of high *BRAF* and *RAF1* expression. Gadoxetic acid–enhanced MRI may facilitate the choice of gene therapy for patients with HCC.

Key Points

- *Incomplete tumor capsule and non-capsule were independent risk factors of HCC with high BRAF and RAF1 expression.*
- *The presence of intratumoral vessels was a potential indicator of high BRAF and RAF1 expression.*
- *Gadoxetic acid-enhanced MRI may be a predictor of efficacy of treatment with sorafenib.*

Keywords Magnetic resonance imaging · Hepatocellular carcinoma · Gene therapy · Gadoxetic acid

Zhi Dong and Kun Huang contributed equally to this work.

Electronic supplementary material The online version of this article (https://doi.org/10.1007/s00330-018-5882-4) contains supplementary material, which is available to authorized users.

✉ Zi-Ping Li
liziping163@163.com

✉ Shi-Ting Feng
fengsht@mail.sysu.edu.cn

[1] Department of Radiology, The First Affiliated Hospital, Sun Yat-Sen University, 58th, The Second Zhongshan Road, Guangzhou 510080, Guangdong, China

[2] Department of Radiology, Guizhou Provincial People's Hospital, No. 83 East Zhongshan Road, Guiyang 550002, Guizhou, China

[3] Department of Pathology, The First Affiliated Hospital, Sun Yat-Sen University, 58th, The Second Zhongshan Road, Guangzhou 510080, Guangdong, China

[4] Faculty of Medicine and Dentistry, University of Western Australia, 35 Stirling Hwy, Crawley, WA 6009, Australia

Abbreviations

ADC	Apparent diffusion coefficient
DWI	Diffusion-weighted image
ECM	Extracellular matrix
HCC	Hepatocellular carcinoma
MMP	Matrix metalloproteinase
OR	Odds ratio
T1WI	T1-weighted image
T2WI	T2-weighted image
$T1_D$%	Percentage of decrease in T1 relaxation time in the hepatocellular phase
$T1_E$	T1 Relaxation time in the hepatocellular phase
$T1_N$	T1 Relaxation time on non-enhanced scan
VEGFR	Vascular endothelial growth factor receptor
VIBE	Volume interpolated breath-hold examination

Introduction

Hepatocellular cancer (HCC) has become a serious threat to human health [1, 2]. To date, drug-targeted therapy is one option for the treatment of advanced HCC not appropriate for surgery or ablation. Sorafenib is the most commonly administrated HCC-targeted drug approved by the Food and Drug Administration (FDA) [3]. The main action site of sorafenib is Raf-1 and B-Raf. It blocks the Ras/Raf/MEK/ERK signaling pathway, directly inhibiting tumor proliferation. It also acts on vascular endothelial growth factor receptor (VEGFR) 2 and VEGFR3, and others, which indirectly inhibit tumor growth through anti-angiogenesis effects [4, 5]. Although drug-targeted therapy can improve the prognosis of some patients with advanced HCC [4–6], not all patients benefit from sorafenib. It was reported that the efficiency of sorafenib was approximately 43% [4]. Differences in treatment outcomes may be attributable to the target gene heterogenicity of HCC [7, 8]. Previous studies have reported that only some cases of HCC were found to have a BRAF-activated mutation and the expression level of VEGF differed among patients [9–11]. More and more studies showed that differences in the expression levels of target genes resulted in response differences in HCC with sorafenib treatment. A recent study showed that HCC patients with overexpressed RAF1 had better treatment effect with sorafenib and longer survival time compared to patients with weak RAF1 expression [12]. Other studies have also reported differences in the treatment effect of drug-targeted therapy in patients with differences in BRAF expression [13, 14]. Finally, HCC patients with overexpressed VEGFR had better treatment effect with sorafenib compared to patients without VEGFR expression [15]. Therefore, in order to achieve the best cost/performance ratio, detection of target gene expression before drug-targeted treatment might become important.

Preoperative gene detection of HCC relies on lesion biopsy. However, biopsy might not reflect the overall tumor due to heterogeneity [16] and exposes the patient to complications such as bleeding and tumor seeding [17, 18]. The hepatobiliary phase image after gadoxetic acid enhancement improves the lesion detection and characterization [19, 20].

Some studies have correlated imaging features and gene expression. Segal et al [21] found a correlation between intratumoral vessels and CDK4, MCM5, and other vascular invasion-related genes. Thaiss et al found a strong correlation between VEGFR-2 and CT perfusion parameters [22]. However, to date, there has been no report focusing on the relationship between MRI features of HCC and *BRAF*, *RAF1*, *VEGFR2*, and *VEGFR3* gene expression.

This study aimed at analyzing which qualitative and quantitative gadoxetic acid–enhanced MR image features were associated with the presence of *BRAF*, *RAF1*, *VEGFR2*, and *VEGFR3* gene expression.

Materials and methods

This study was conducted in accordance with ethical guidelines for human research and was compliant with the Health Insurance Portability and Accountability Act (HIPAA); as such, the study received institutional review board (IRB) or ethical committee approval, and written informed consent was obtained from all patients in the study.

Study population

We retrospectively analyzed 91 patients with HCC (age 25–84, mean 53.9 ± 12 years; males/females, 81/10 evaluated in our hospital from November 2011 to August 2016. The inclusion criteria were as follows: (1) postoperative pathology-confirmed HCC; (2) solitary lesion; (3) preoperative gadoxetic acid–enhanced MRI examination; (4) no distant metastases; (5) operation performed within 2 weeks after MRI examination; (6) no treatment received for HCC before the MR examination and surgical resection.

The exclusion criteria were as follows: (1) absence of MRI or absence of injection; (2) history of other malignancies; (3) incomplete clinical or pathological information; (4) poor-quality MRI that could not meet the requirement for evaluation of image features (Fig.1).

MRI

All patients underwent upper abdominal MR examination using a 3 T Magnetom trio (Siemens Healthineers). The main sequences and parameters were as follows: half-Fourier single-shot turbo spin-echo sequence for localization, T1-weighted image (T1WI), T2-weighted image (T2WI),

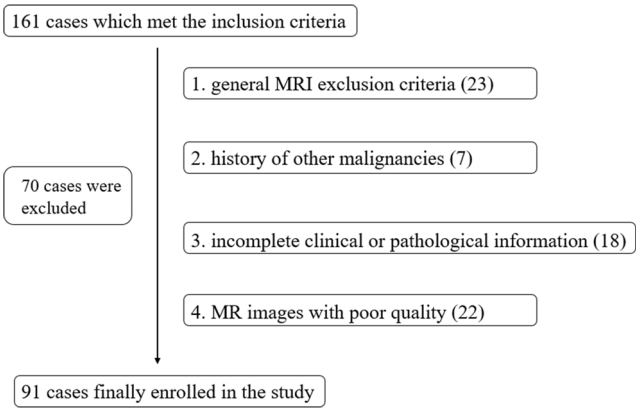

Fig. 1 Flow chart of inclusion and exclusion of patients enrolled

diffusion-weighted image (DWI, b = 50, 800 s/mm^2), T1 mapping, and dynamic gadoxetic acid–enhanced sequence using volume interpolated breath-hold examination (VIBE) T1-weighted gradient echo imaging with fat suppression. The injection volume of contrast medium was 0.025 mmol/kg at a rate of 2 mL/s; then, the catheter was flushed with 30 mL 0.9% sodium chloride solution (NaCl), at the same rate of 2 mL/s. The dynamic gadoxetic acid–enhanced sequence began 13–25 s after contrast agent injection using VIBE T1-weighted gradient echo imaging with fat suppression. The arterial, portal venous, and equilibrium phases were acquired at 13–43 s, 50–80s, and 95–120 s, respectively. The hepatic phase was acquired 20 min after contrast agent injection. Specific MR sequences and parameters are shown in supplementary Table 1.

Image analysis

The images were evaluated by two experienced radiologists (6 years and 15 years of experience respectively) who were blinded to the pathological results. The qualitative image features (tumor thrombus, signal intensity, tumor capsule status, tumor margins, intratumoral vessels, peritumoral enhancement, and peritumoral hypointensity) were confirmed by consensus between the two radiologists. The quantitative characteristics were obtained by averaging the two evaluation results.

Assessment of qualitative features [23–25] (Figs. 2, 3): (1) tumor thrombus: filling defect in the portal or hepatic vein with dominant enhancement in the arterial phase and washout in the portal venous phase; (2) signal intensity: assessment of the uniformity of tumor signal intensity on transverse T2WI; (3) tumor capsule: the thin rim with hyperintensity at the edge of tumor in the delayed phase was considered to be the tumor capsule. According to the existence of capsule sign, tumors were defined as capsular or non-capsular. Capsular tumors were further divided into having a complete or incomplete capsule; (4) tumor margins: according to the morphology in the hepatobiliary phase, the tumors were divided into four types: smooth solitary nodule, protruding nodule, fusion of multiple nodules, and irregular infiltration type; (5) intratumoral vessels: visible vessels in the tumor in the arterial phase; (6) peritumoral enhancement: the patchy or crescent-shaped area around the tumor with hyperintensity in the arterial phase and isointensity in the portal phase and equilibrium phase; (7) peritumoral hypointensity: the irregular or wedge-shaped area around the tumor with hypointensity in the hepatobiliary phase.

The quantitative characteristics included the maximum diameter of the tumor, apparent diffusion coefficient (ADC) value, and percentage of decrease in T1 ($T1_D$%). The maximum diameter of the tumor was measured in the hepatobiliary phase, based on axial and coronal images. The ADC value, T1 relaxation time on non-enhanced scan ($T1_N$), and the hepatocellular phase ($T1_E$) were obtained at the level of the tumor's solid component, avoiding necrosis, vessels, and artifacts, with the region of interest being as large as possible. $T1_{D\%}$ was calculated as follows: $T1_{D\%} = (T1_N - T1_E)/T1_N$.

Gene expression analysis

Sample

Gross samples were surgically removed from the patients with HCC. The intratumoral specimens were obtained from seven sites in the original lesion avoiding necrotic and bleeding areas. All the specimens were subjected to immunohistochemical staining of Raf-1, B-Raf, VEGFR2, and VEGFR3.

Result interpretation

To interpret a positive sign, we considered that Raf-1 shows yellow/brown staining of the cell membrane and cytoplasm, B-Raf shows yellow/brown staining of the nucleus, membrane, and cytoplasm, VEGFR2 shows yellow/brown staining of the cell membrane, and VEGFR3 shows yellow/brown staining of the cell membrane (Fig. 4).

The specimen slides were independently read by two pathologists (10 years and 21 years of experience, respectively), and the average score was regarded as the final result. The scoring method was two-staged and the score was the product of staining density and positive cell counting. The mean score of seven sampling points was considered to be the scoring result of each lesion. The staining density was classified as follows: negative, 0 point; faint yellow, 1 point; yellow, 2 points; brown or dark brown, 3 points. The positive cell count was the percentage of positive cells in 100 cells in × 10 high magnification, which was divided into four categories: 0–10%, 0 point; 11–25%, 1 point; 26–50%, 2 points; 51–75%, 3 points; > 75%, 4 points. Considering the median score as a

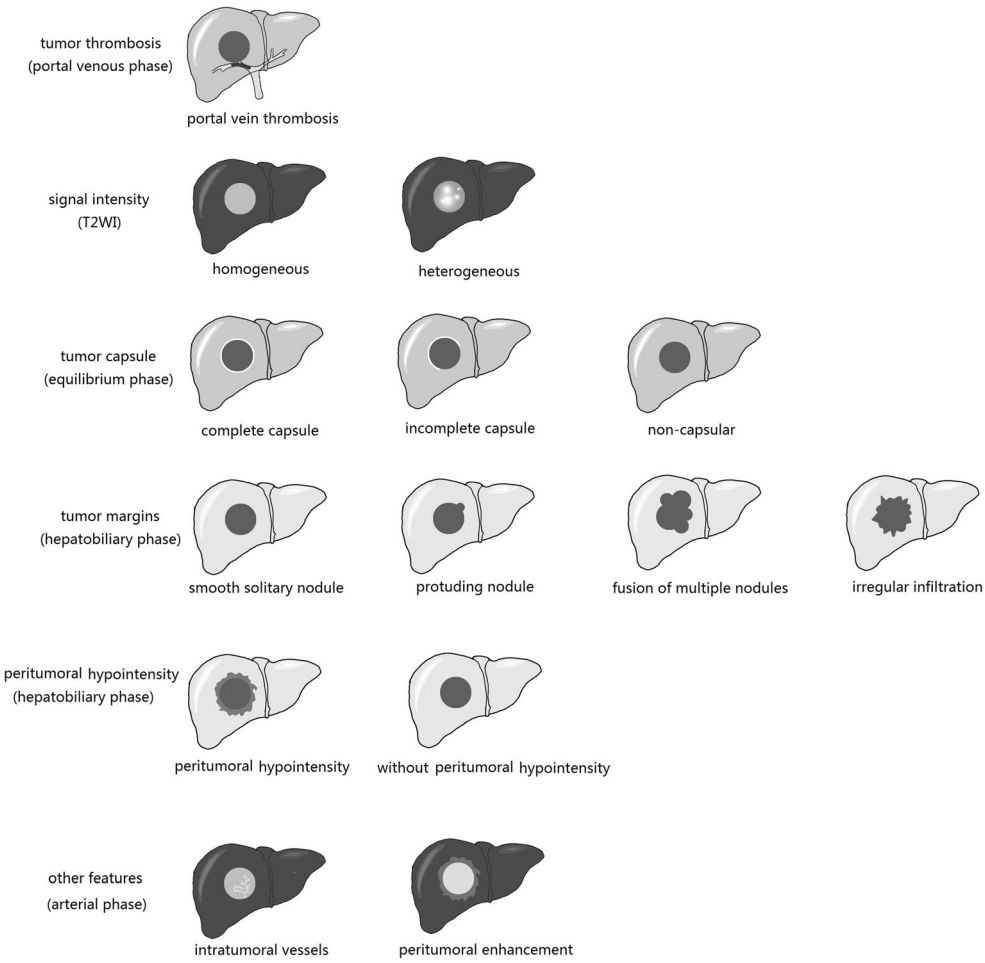

Fig. 2 Qualitative features of HCC. Assessment of qualitative features including tumor thrombus, signal intensity, tumor capsule, tumor margins, intratumoral vascular, peritumoral enhancement, and peritumoral hypointensity

dividing line, the gene expression level was divided into a high-expression group and a low-expression group [11].

Statistical analysis

The interobserver agreement between the two experienced radiologists and the two pathologists were evaluated using the kappa agreement test. Non-parametric tests were used to evaluate the differences among different MRI qualitative characteristics groups. The multiple MRI feature groups were analyzed with the Kruskal-Wallis *H* test, and comparisons between every two groups were also performed. Binary MRI features were analyzed with the Mann-Whitney *U* test. The correlation between quantitative MRI features and gene expression was analyzed with Spearman's correlation.

Variables with statistical difference in the univariate analysis were entered in a logistic regression model, using the forward (condition) method for screening, with 0.05 as the inclusion criterion and 0.1 as the exclusion criterion. $P < 0.05$ indicated statistical significance.

All statistical analyses were performed using SPSS 20.0 (IBM Corp.).

Results

Gene expression results

Gene expression scores of *BRAF*, *RAF1*, *VEGFR2*, and *VEGFR3* were recorded and compared with imaging features in each patient (Fig. 5). The median scores were 4.00, 8.00, 1.00, and 2.00, respectively (Fig. 6). The inter-reader agreement is shown in supplementary Table 2.

Qualitative MRI features

Tumor thrombi were found in 10 cases (11%), while no thrombus was found in the other 81 cases (89%); the signal intensity of the tumor was homogeneous in 24 cases (26%) and heterogeneous in 67 cases (74%); there were 16 tumors with complete capsules (18%) and 62 tumors with incomplete capsules (68%); the other 13 tumors had no capsule (14%). There were 15 cases of smooth solitary nodules (16%), 50 cases of protruding nodules (55%), and 26 cases where the tumors were a fusion of multiple nodules. There were 43 cases with intratumoral vessels (47%) and 48 cases without (53%).

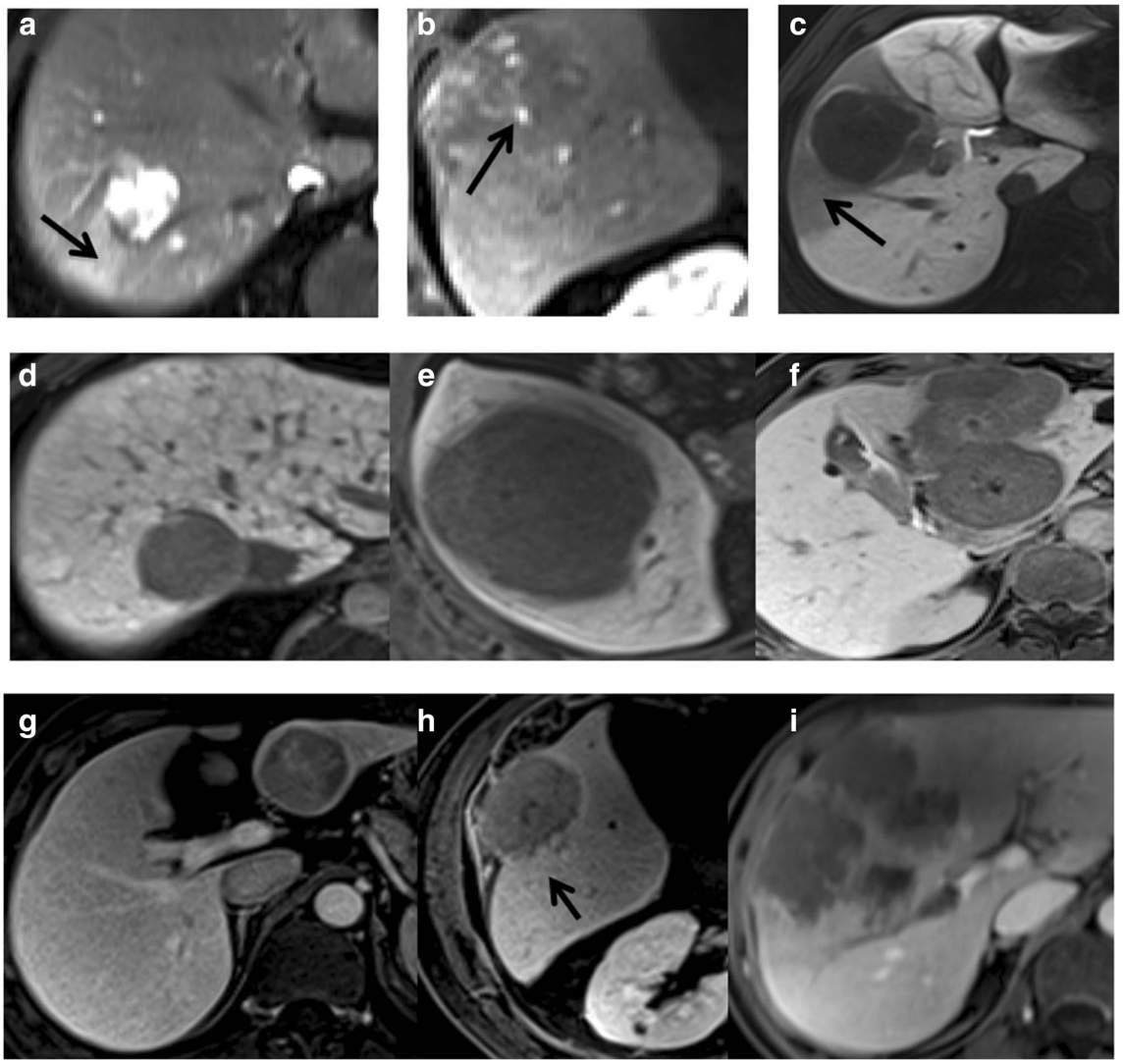

Fig. 3 MR image features in HCC patients. **a** Peritumoral enhancement (black arrow); **b** intratumoral vessel (black arrow); **c** peritumoral hypointensity (black arrow); **d**–**f** show tumor margins including smooth nodule, protruding nodule and fusion of multiple nodules, respectively; **g**–**i** show tumor capsule status: complete, incomplete capsule and non-capsule

There were 29 cases with peritumoral enhancement (32%), and 62 cases without (68%). Peritumoral hypointensity was found in 29 cases (32%), while no peritumoral hypointensity was found in the other 62 cases (68%). The interobserver agreement of qualitative MRI features between the two experienced radiologists is shown in Table 1.

Quantitative MRI features

The maximum diameters of 91 HCCs were measured, ranging from 17.00 to 168.00 mm; the average value was 52.30 ± 34.00 mm. Sixty-five cases underwent DWI and the ADC values were measured. The range of ADC values was (0.54–2.16) × 10^{-3} mm^2/s; the average value was (1.05 ± 0.27) × 10^{-3} mm^2/s. Thirty-six cases underwent T1 mapping and the T1 values were measured. The range of $T1_{D\%}$ was 0.2–0.9, and the average value was 0.39 ± 0.15.

Correlation analysis

BRAF gene

Univariate analysis showed that the *BRAF* gene expression level was statistically different among the complete, incomplete, and no-capsule groups ($p = 0.000$), and between the intratumoral vessel group and the no-intratumoral vessel group ($p = 0.002$). No statistical difference was found among the other qualitative MRI feature groups (Table 2). There was no statistical association between the *BRAF* gene expression level and quantitative MRI features ($p > 0.05$) (Table 3).

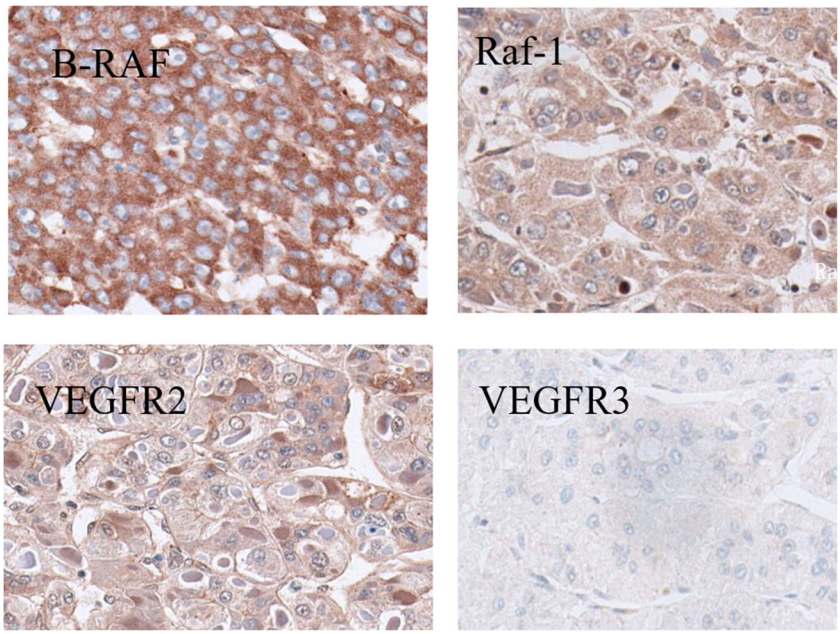

Fig. 4 Immunohistochemical staining of *BRAF*, *RAF1*, *VEGFR2*, and *VEGFR3*. B-Raf shows yellow/brown staining of the nucleus, membrane, and cytoplasm. Raf-1 shows yellow/brown staining of the cell membrane and cytoplasm. VEGFR2 shows yellow/brown staining of the cell membrane, and VEGFR3 shows yellow/brown staining of the cell membrane

Multivariate analysis showed that the tumor capsule was an independent factor of *BRAF* expression ($p = 0.006$). The *BRAF* gene expression level in the no-capsule group was higher than that in the complete capsule group ($p = 0.004$, OR = 15.750, 95% CI: 2.373–104.537). The *BRAF* gene expression level in the incomplete capsule group was also higher than that in the complete capsule group ($p = 0.002$, OR = 11.870, 95% CI: 2.473–56.975). There was no statistical difference between the no-capsule group and the incomplete capsule group ($p = 0.666$) (Table 4). The presence of

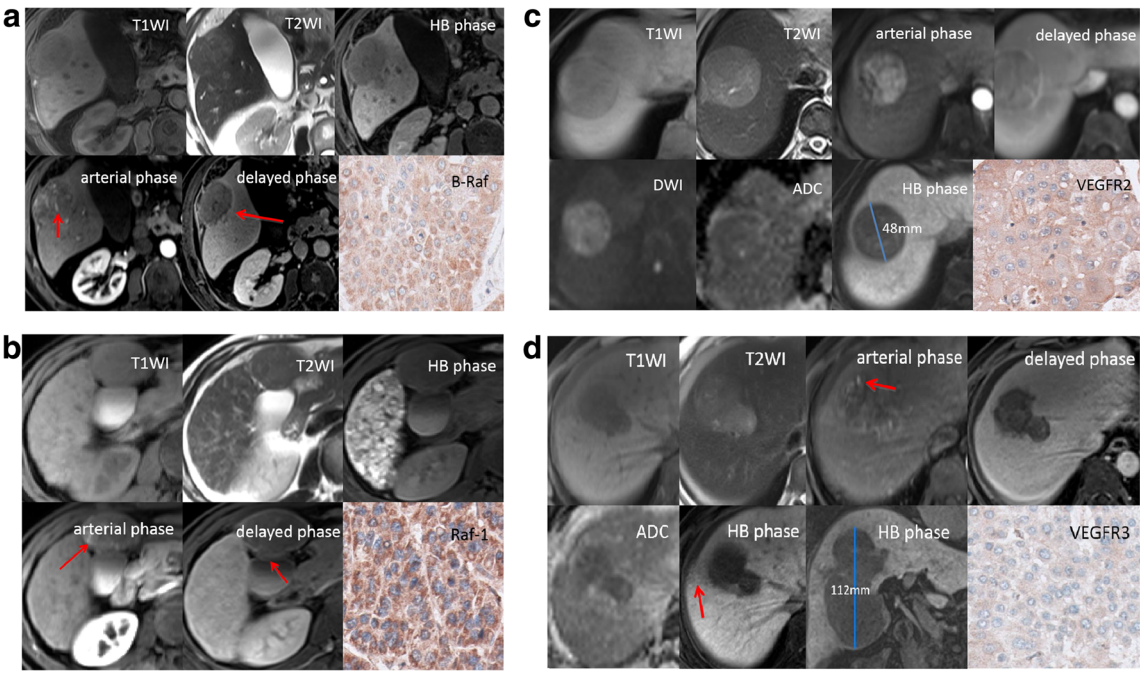

Fig. 5 HCCs with *BRAF*, *RAF1*, *VEGFR2*, and *VEGFR3* expression. **a** A 65-year-old man. Arterial phase shows visible intratumoral vessels (arrow). Delayed phase shows the tumor capsule is incomplete (arrow). Hepatobiliary (HB) phase shows that the tumor is nodule with focal protrusion. The *BRAF* expression score is 8. **b** A 42-year-old man. Arterial phase shows visible intratumoral vessel (arrow); the tumor capsule is incomplete in the delayed phase (arrow). The *RAF1* expression score is 12. **c** A 68-year-old woman. Complete tumor capsule is seen in the delayed phase. The tumor is hyperintense in DWI, and hypointense in the apparent diffusion coefficient (ADC) image. HB phase shows that the tumor is a smooth nodular type. The *VEGFR2* expression score is 1. **d** A 48-year-old man. Arterial phase shows visible intratumoral vessels (arrow). HB phase shows that the tumor is a fusion of multiple nodules, with peritumoral hypointensity. The *VEGFR3* expression score is 1

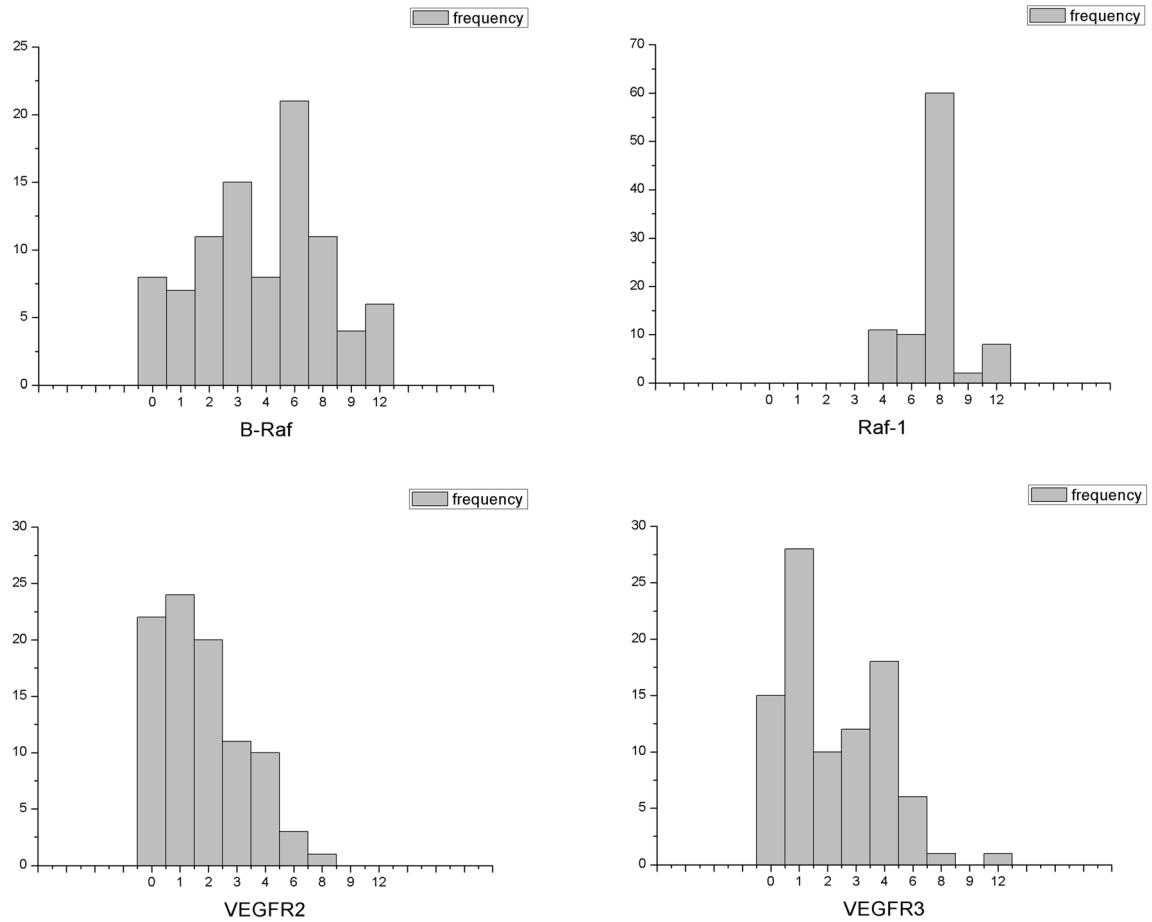

Fig. 6 Gene expression score distribution of *BRAF*, *RAF1*, *VEGFR2*, and *VEGFR3*

intratumoral vessels was not an independent factor of *BRAF* expression ($p = 0.127$).

RAF1 gene

Univariate analysis showed that the *RAF1* gene expression level was statistically different among the complete, incomplete, and no-capsule groups ($p = 0.001$), and between the intratumoral vessel group and the no-intratumoral vessel group ($p = 0.013$). No statistical difference was found among the other qualitative MRI feature groups (Table 2). There was no statistical association between the *RAF1* gene expression level and quantitative MRI features ($p > 0.05$) (Table 3).

Multivariate analysis showed that the tumor capsule was an independent factor of *RAF1* expression ($p = 0.001$). The *RAF1* expression level in the no-capsule group was higher than that in the complete capsule group ($p = 0.040$, OR = 5.556, 95% CI 1.078–28.635). The *RAF1* gene expression level in the incomplete capsule group was also higher than that in the complete capsule group ($p < 0.001$, OR = 11.250, 95% CI 3.206–39.474). There was no statistical difference between the no-capsule group and the incomplete capsule group ($p = 0.353$) (Table 4). The presence of intratumoral vessels was not an independent factor of *RAF1* expression ($p = 0.320$).

VEGFR2 gene

Univariate analysis showed that no statistical difference was found in the *VEGFR2* gene expression level among all qualitative MRI feature groups ($p > 0.05$) (Table 2). Moreover, there was no statistical association between the *VEGFR2* gene expression level and quantitative MRI features ($p > 0.05$) (Table 3).

VEGFR3 gene

Univariate analysis showed that the *VEGFR3* gene expression level was statistically different among the complete, incomplete, and no-capsule groups ($p = 0.030$). However, comparisons between every two groups showed no significant difference ($p > 0.05$) (Table 5). No statistical difference was found in the *VEGFR3* gene expression level among the qualitative MRI feature groups ($p > 0.05$) (Table 2). Moreover, there was no statistical association between the *VEGFR3* gene expression level and quantitative MRI features ($p > 0.05$) (Table 3).

Table 1 Interobserver agreement in qualitative MR image features

MRI features (91 cases)	Observer A (15-year experience)	Observer B (6-year experience)	Agreement test (kappa value)
Tumor thrombus			1.000
Yes	10	10	
None	81	81	
Signal intensity			0.831
homogeneous	28	35	
heterogeneous	63	56	
Tumor capsule			0.649
Complete	16	21	
Incomplete	62	59	
None	13	11	
Tumor margins			0.713
Smooth solitary nodule	15	15	
Protruding nodule	50	45	
Fusion of multiple nodules	26	28	
Intratumoral vascular			0.780
Yes	43	45	
None	48	46	
Peritumoral enhancement			0.670
Yes	29	37	
None	62	54	
Peritumoral hypointensity			0.734
Yes	29	34	
None	62	57	

Discussion

In this study, we found that there was a relationship between capsule appearance and presence of intratumoral vessels on one hand, and genetic profile of the tumor on the other hand. This is of potential interest to predict the quality of response to treatment with sorafenib as there is increasing evidence that gene expression interferes with the response to sorafenib treatment in patients [3–15]. We found that the appearance of the tumor capsule is an independent predictor of *BRAF* and *RAF1* expression. HCC patients who have incomplete tumor capsule or no capsule have higher *BRAF* and *RAF1* gene expression compared with patients with complete tumor capsule. The presence of intratumoral vessels also indicates higher *BRAF* and *RAF1* expression. B-Raf and Raf1 mainly act downstream of the ERK/MAPK pathway, regulating nuclear factors by cascade amplification, and the abnormal activation of this pathway accelerates the proliferation and differentiation of HCC cells [26–29]. *RAF* gene also promotes the expression of matrix metalloproteinases (MMPs), which alters the adhesion of tumor cells, degrades the extracellular matrix (ECM) and basement membrane, and promotes invasion and metastasis of tumors [30, 31]. Previous studies have shown that MMP2-positive HCCs often have no capsules, and MMP9-positive HCCs have incomplete capsules or are non-encapsulated [32, 33]. Accordingly, HCCs with high expression of *BRAF* and *RAF1* tend to have rapid proliferation and growth, and the surrounding hepatic tissue has insufficient response time to form a complete capsule that limits tumor growth; besides, high expression of *BRAF* and *RAF1* elevates MMPs expression, which promotes capsule destruction. Therefore, the integrity of the tumor capsule can reflect the expression level of the *BRAF* and *RAF1* genes.

In univariate analysis, we found that the presence of intratumoral vessels is closely related to *BRAF* and *RAF1* expression. HCCs with intratumoral vessels had higher expression of *BRAF* and *RAF1* than those without. This may be explained by the role of *BRAF* and *RAF1* genes in tumor angiogenesis mediated by various growth factors [34, 35]. Besides, MMP-regulated extracellular matrix remodeling plays a critical role in tumor angiogenesis because the formation of the tumor vessel lumen only occurs in the process of extracellular matrix remodeling [36, 37]. Since the expression of MMPs is regulated and controlled by the *RAF* genes, tumor angiogenesis is indirectly monitored by the *RAF* genes. However, according to the multivariate analysis, the presence of intratumoral vessels was not an independent factor of *BRAF* and *RAF1* gene expression. In multivariate analysis, we

Table 2 Comparison between qualitative magnetic resonance imaging (MRI) features and gene expression scores of HCC

MRI features	*BRAF* *p* value	*RAF1* *p* value	*VEGFR2* *p* value	*VEGFR3* *p* value
Tumor thrombus	0.434	0.092	0.762	0.322
Yes ($n = 10$)				
None ($n = 81$)				
Signal intensity	0.451	0.130	0.955	0.796
Homogeneous ($n = 24$)				
Heterogeneous ($n = 67$)				
Tumor capsule	*0.000*	*0.001*	0.274	*0.030*
Complete ($n = 16$)				
Incomplete ($n = 62$)				
None ($n = 13$)				
Tumor margins	0.300	0.545	0.793	0.784
Smooth solitary nodule ($n = 15$)				
Protruding nodule ($n = 50$)				
Fusion of multiple nodules ($n = 26$)				
Intratumoral vascular	*0.002*	*0.013*	0.973	0.221
Yes ($n = 43$)				
None ($n = 48$)				
Peritumoral enhancement	0.402	0.107	0.389	0.226
Yes ($n = 29$)				
None ($n = 62$)				
Peritumoral hypointensity	0.282	0.218	0.562	0.231
Yes ($n = 29$)				
None ($n = 62$)				

Gene expression level of *BRAF*, *RAF1*, and *VEGFR3* was statistically different among the complete, incomplete, and no-capsule groups (p = 0.000, 0.001, and 0.030, respectively); gene expression level of *BRAF* and *RAF1* was statistically different between the intratumoral vessel group and the no-intratumoral vessel group (p = 0.002, 0.013, respectively)

included both the presence of tumor capsule and of intratumoral vessels, and we found that the status of tumor capsule was an independent factor of *BRAF* and *RAF1* expression, while intratumoral vessel was not. The presence of tumor capsule had greater influence on the expression of the *BRAF* and *RAF1* genes than the presence of intratumoral vessels. When the tumor had both an incomplete capsule (or no capsule) and intratumoral vessels, the expression of the *BRAF* and *RAF1* genes tended to be higher. When the tumor had an incomplete capsule (or no capsule) but no intratumoral vessels, there was still a high probability of strongly expressed *BRAF* and *RAF1* genes. However, when the tumor had a complete capsule, the possibility of high expression of the *BRAF* and *RAF1* genes was very low, even in the presence of intratumoral vessels.

In our study, the existence of visible blood vessels on enhanced MRI had no significant correlation with the expression levels of *VEGFR2*, and *VEGFR3*. This is because *VEGFR2*, and *VEGFR3* reflect the proliferation of microvasculature, which may only be observed pathologically, whereas the intratumoral vessels seen on MRI merely represent parts of the tumor vessels that are distorted and widened, and cannot reflect the actual number and density of the tumoral microvasculature [38]. Additionally, our study showed that the expression of *VEGFR3* in the three tumor capsule groups was significantly different. However, pair comparisons showed no statistically significant difference between any two groups. This may be attributable to the small sample size, and the different level of *VEGFR3* expression between groups cannot be clearly demonstrated.

Huang et al [39] assessed the HCC *VEGF* expression level with the ADC value and found a negative correlation between the ADC value and the *VEGF* expression level. However, we analyzed the relationship between the ADC value and the expression of some HCC genes and found no significant correlation between ADC values and *VEGFR2*, and *VEGFR3* expression. The difference may be caused by potential selection bias due to pathological sampling.

To our best knowledge, there are no studies focusing on the correlation between HCC gene expression and T1 relaxation time of HCC. In our study, we found that the percentage of decrease in T1 ($T1_D$%) had no significant correlation with *BRAF*, *RAF1*, *VEGFR2*, and *VEGFR3* expression. One explanation could be that the uptake of gadoxetic acid in HCC is affected by the level of OATPs on tumor cells [40], and there is no direct correlation between OATPs and the expression levels of *BRAF*, *RAF1*, *VEGFR2*, and *VEGFR3*. Therefore,

Table 3 Correlation between quantitative MRI features and gene expression scores

MRI features	*BRAF*		*RAF1*		*VEGFR2*		*VEGFR3*	
	Correlation coefficient	*p* value	Correlation coefficient	*p* value	Correlation coefficient	*p* value	Correlation coefficient	*p* value
Maximum diameter (mm) ($n = 91$)	0.077	0.466	- 0.019	0.855	- 0.057	0.588	- 0.033	0.759
ADC ($\times 10^{-3}$ mm^2/s) ($n = 65$)	0.127	0.300	0.050	0.685	0.101	0.410	0.113	0.359
$T1_{D\%}$ ($n = 65$)	0.192	0.262	0.082	0.635	0.044	0.800	- 0.145	0.398

ADC apparent diffusion coefficient, $T1_{D\%}$ percentage of decrease in T1

Table 4 Logistic regression analysis of factors influencing *BRAF* and *RAF1* expression levels

Variable	*BRAF* gene			*RAF1* gene		
	p value	OR	95% CI	*p* value	OR	95% CI
Tumor capsule	0.006			0.001		
complete vs incomplete (*n* = 16) (*n* = 62)	0.002	11.870	2.473, 56.975	0.000	11.250	3.206, 39.474
complete vs none (*n* = 16) (*n* = 13)	0.004	15.750	2.373, 104.537	0.040	5.556	1.078, 28.635
none vs incomplete (*n* = 13) (*n* = 62)	0.666	0.754	0.208, 2.726	0.353	2.025	0.457, 8.973

OR odds ratio

BRAF, *RAF1*, *VEGFR2*, and *VEGFR3* expression has no influence on the uptake of gadoxetic acid in HCC.

As previously reported, sorafenib mainly acts on the *BRAF* and *RAF1* genes to inhibit the Ras/Raf/MEK/ERK signaling pathway and prevent neo-angiogenesis by acting on VEGFR, thus retarding tumor growth [4, 5]. Therefore, patients with high expression of these genes may have a better treatment effect with sorafenib. As our study showed that the presence of an incomplete tumor capsule or no capsule and intratumoral vessels suggested high expression of *BRAF* and *RAF1*, a better efficacy of sorafenib treatment can be expected in this case.

There are some limitations. First, there may have been potential selection bias due to pathological sampling. Second, the study population of quantitative MRI features was relatively small, and T1 mapping and ADC evaluation were not available in all patients. Further studies with larger and multicentric cohorts are needed. Third, the results from our present study cannot differentiate *RAF1* from *BRAF* using MR imaging features.

Conclusion

Sorafenib is a targeted drug whose main action sites are Raf-1 and B-Raf and VEGFR 2 and VEGFR3. The presence of incomplete capsule or intratumoral vessels and the absence of capsule are potential indicators of high *BRAF* and *RAF1* expression and potential predictors of sorafenib efficacy. However, this hypothesis still requires verification by larger samples in multiple centers in further study, which is in progress.

Table 5 Comparison of *VEGFR3* expression levels among the tumor capsule status groups

Variable	Statistics	*p* value
Tumor capsule		
Complete vs incomplete (*n* = 16) (*n* = 62)	2.704	1.000
Complete vs none (*n* = 16) (*n* = 13)	16.802	0.154
None vs incomplete (*n* = 13) (*n* = 62)	− 14.098	0.099

Funding This work was funded by the National Natural Science Foundation of China (81771908, 81571750, 81770654).

Compliance with ethical standards

Guarantor The scientific guarantor of this publication is Zi-Ping Li.

Conflict of interest The authors of this manuscript declare no relationships with any companies, whose products or services may be related to the subject matter of the article.

Statistics and biometry One of the authors has significant statistical expertise.

Informed consent Written informed consent was obtained from all subjects (patients) in this study.

Ethical approval Institutional Review Board approval was obtained.

Methodology
- retrospective
- observational
- performed at one institution

References

1. Torre LA, Bray F, Siegel RL, Ferlay J, Lortet-Tieulent J, Jemal A (2015) Global cancer statistics, 2012. CA Cancer J Clin 65(2):87–108
2. Chen W, Zheng R, Baade PD et al (2016) Cancer statistics in China, 2015. CA Cancer J Clin 66(2):115–132
3. Kudo M (2012) Treatment of advanced hepatocellular carcinoma with emphasis on hepatic arterial infusion chemotherapy and molecular targeted therapy. Liver Cancer 1(2):62–70
4. Llovet JM, Ricci S, Mazzaferro V et al (2008) Sorafenib in advanced hepatocellular carcinoma. N Engl J Med 359(4):378–390
5. Cheng AL, Kang YK, Chen Z et al (2009) Efficacy and safety of Sorafenib in patients in the Asia-Pacific region with advanced hepatocellular carcinoma: a phase III randomised, double-blind, placebo-controlled trial. Lancet Oncol 10(1):25–34
6. Cammà C, Cabibbo G, Petta S et al (2013) Cost-effectiveness of sorafenib treatment in field practice for patients with hepatocellular carcinoma. Hepatology 57(3):1046–1054

7. Burrell RA, Mcgranahan N, Bartek J, Swanton C (2013) The causes and consequences of genetic heterogeneity in cancer evolution. Nature 501(7467):338–345
8. Bedard PL, Hansen AR, Ratain MJ, Siu LL (2013) Tumour heterogeneity in the clinic. Nature 501(7467):355–364
9. Colombino M, Sperlongano P, Izzo F et al (2012) BRAF and PIK3CA genes are somatically mutated in hepatocellular carcinoma among patients from South Italy. Cell Death Dis 3:e259
10. Chiang DY, Villanueva A, Hoshida Y et al (2008) Focal gains of VEGFA and molecular classification of hepatocellular carcinoma. Cancer Res 68(16):6779–6788
11. Kan Z, Zheng H, Liu X et al (2013) Whole-genome sequencing identifies recurrent mutations in hepatocellular carcinoma. Genome Res 23(9):1422–1433
12. Lei J, Zhong J, Hao J et al (2016) Hepatocellular carcinoma cases with high levels of c-Raf-1 expression may benefit from postoperative adjuvant sorafenib after hepatic resection even with high risk of recurrence. Oncotarget 7(27):42598–42607
13. Wilhelm SM, Carter C, Tang L et al (2004) BAY 43-9006 exhibits broad spectrum oral antitumor activity and targets the RAF/MEK/ERK pathway and receptor tyrosine kinases involved in tumor progression and angiogenesis. Cancer Res 64(19):7099–7109
14. Wan PT, Garnett MJ, Roe SM et al (2004) Mechanism of activation of the RAF-ERK signaling pathway by oncogenic mutations of B-RAF. Cell 116(6):855–867
15. Peng S, Wang Y, Peng H et al (2014) Autocrine vascular endothelial growth factor signaling promotes cell proliferation and modulates sorafenib treatment efficacy in hepatocellular carcinoma. Hepatology 60(4):1264–1277
16. Friemel J, Rechsteiner M, Frick L et al (2015) Intratumor heterogeneity in hepatocellular carcinoma. Clin Cancer Res 21(8):1951–1961
17. Stigliano R, Marelli L, Yu D, Davies N, Patch D, Burroughs AK (2007) Seeding following percutaneous diagnostic and therapeutic approaches for hepatocellular carcinoma. What is the risk and the outcome? Seeding risk for percutaneous approach of HCC. Cancer Treat Rev 33(5):437–447
18. Silva MA, Hegab B, Hyde C, Guo B, Buckels JA, Mirza DF (2008) Needle track seeding following biopsy of liver lesions in the diagnosis of hepatocellular cancer: a systematic review and meta-analysis. Gut 57(11):1592–1596
19. Ahn SS, Kim MJ, Lim JS, Hong HS, Chung YE, Choi JYl (2010) Added value of gadoxetic acid-enhanced hepatobiliary phase MR imaging in the diagnosis of hepatocellular carcinoma. Radiology 255(2):459–466
20. Kogita S, Imai Y, Okada M et al (2010) Gd-EOB-DTPA-enhanced magnetic resonance images of hepatocellular carcinoma: correlation with histological grading and portal blood flow. Eur Radiol 20(10):2405–2413
21. Segal E, Sirlin CB, Ooi C et al (2007) Decoding global gene expression programs in liver cancer by noninvasive imaging. Nat Biotechnol 25(6):675–680
22. Thaiss WM, Kaufmann S, Kloth C, Nikolaou K, Bösmüller H, Horger M (2016) VEGFR-2 expression in HCC, dysplastic and regenerative liver nodules, and correlation with pre-biopsy dynamic contrast enhanced CT. Eur J Radiol 85(11):2036–2041
23. Purysko AS, Remer EM, Coppa CP, Leão Filho HM, Thupili CR, Veniero JC (2012) LI-RADS: a case-based review of the new categorization of liver findings in patients with end-stage liver disease. Radiographics 32:1977–1995
24. Choi JY, Lee JM, Sirlin CB (2014) CT and MR imaging diagnosis and staging of hepatocellular carcinoma: part I. development, growth, and spread: key pathologic and imaging aspects. Radiology 272(3):635–654
25. Elsayes KM, Hooker JC, Agrons MM et al (2017) 2017 version of LI-RADS for CT and MR imaging: an update. Radiographics 37(7):1994–2017
26. Schreck R, Rapp UR (2006) Raf kinases: oncogenesis and drug discovery. Int J Cancer 119(10):2261–2271
27. Leicht DT, Balan V, Kaplun A et al (2007) Raf kinases: function, regulation and role in human cancer. Biochim Biophys Acta 1773(8):1196–1212
28. Zebisch A, Troppmair J (2006) Back to the roots: the remarkable RAF oncogene story. Cell Mol Life Sci 63(11):1314–1330
29. Wellbrock C, Karasarides M, Marais R (2004) The RAF proteins take centre stage. Nat Rev Mol Cell Biol 5(11):875–885
30. Yue P, Gao ZH, Xue X et al (2011) Des-gamma-carboxyl prothrombin induces matrix metalloproteinase activity in hepatocellular carcinoma cells by involving the ERK1/2 MAPK signalling pathway. Eur J Cancer 47(7):1115–1124
31. Vu TH, Werb Z (2000) Matrix metalloproteinases: effectors of development and normal physiology. Genes Dev 14(17):2123–2133
32. Wang B, Ding YM, Fan P, Wang B, Xu JH, Wang WX (2014) Expression and significance of MMP2 and HIF-1alpha in hepatocellular carcinoma. Oncol Lett 8(2):539–546
33. Sun MH, Han XC, Jia MK et al (2005) Expressions of inducible nitric oxide synthase and matrix metalloproteinase-9 and their effects on angiogenesis and progression of hepatocellular carcinoma. World J Gastroenterol 11(38):5931–5937
34. McPhillips F, Mullen P, MacLeod KG et al (2006) Raf-1 is the predominant Raf isoform that mediates growth factor-stimulated growth in ovarian cancer cells. Carcinogenesis 27(4):729–739
35. Galabova-Kovacs G, Matzen D, Piazzolla D et al (2006) Essential role of B-Raf in ERK activation during extraembryonic development. Proc Natl Acad Sci U S A 103(5):1325–1330
36. Senger DR, Davis GE (2011) Angiogenesis. Cold Spring Harb Perspect Biol 3(8):a005090
37. Beliveau A, Mott JD, Lo A et al (2010) Raf-induced MMP9 disrupts tissue architecture of human breast cells in three-dimensional culture and is necessary for tumor growth in vivo. Genes Dev 24(24):2800–2811
38. Lee JH, Lee JM, Kim SJ et al (2012) Enhancement patterns of hepatocellular carcinomas on multiphasic multidetector row CT: comparison with pathological differentiation. Br J Radiol 85(1017):E573–E583
39. Huang Z, Meng X, Xiu J et al (2014) MR imaging in hepatocellular carcinoma: correlations between MRI features and molecular marker VEGF. Med Oncol 31(12):313
40. Narita M, Hatano E, Arizono S et al (2009) Expression of OATP1B3 determines uptake of Gd-EOB-DTPA in hepatocellular carcinoma. J Gastroenterol 44(7):793–798